Supplemental information for "Sub-lithospheric small scale convection — a mechanism for collision zone magmatism"

L. Kaislaniemi[a,*], J. van Hunen[a], M. B. Allen[a], I. Neill[a]

[a] Department of Earth Sciences, Durham University, Science Labs, Durham, DH1 3LE, United Kingdom

Contents

1 Equations and numerical modelling

We solve the non-dimensional equations of conservation of mass, momentum, and energy using finite element mantle convection code Citcom (Moresi and Gurnis, 1996; Zhong et al., 2000). The extended Boussinesq approximation (Christensen and Yuen, 1985) is used to account for shear heating, adiabatic heating, and the latent heat of melting. Equations applied are:

$$\nabla \cdot \mathbf{u} = 0\,, \tag{1}$$

$$\nabla \left[\eta(\nabla \mathbf{u} + \nabla^{\mathrm{T}}\mathbf{u})\right] - \nabla \cdot P = -RaT \cdot \hat{\mathbf{e}}_{\mathbf{z}} - RbF \cdot \hat{\mathbf{e}}_{\mathbf{z}}\,, \text{ and} \tag{2}$$

$$\frac{\partial T}{\partial t} + \mathbf{u} \cdot \nabla T = \nabla^2 T + L\left(\frac{\partial F}{\partial t} + \mathbf{u} \cdot \nabla F\right) + \frac{Di}{Ra}\eta\dot{\epsilon}^2 + Di(T + T_s)u_z\,, \tag{3}$$

where $\mathbf{u}$ is the velocity vector, η viscosity, P deviatoric pressure, Ra thermal Rayleigh number, T temperature,$\hat{\mathbf{e}}_{\mathbf{z}}$ vertical unit vector, Rb compositional (depletion) Rayleigh number, F depletion, t time, L latent heat of melt, Di dissipation number, ϵ strain, and T_s the surface temperature. Used values of all the parameters are given in Table 1. The advection of compositional field (depletion and water content) and heat is implemented using the marker-in-cell method (e.g. Gerya and Yuen, 2003) with a second order Runge-Kutta scheme.

*Corresponding author. E-mail address: lars.kaislaniemi@iki.fi

Rayleigh numbers are defined as

$$Ra = \frac{\alpha T_0 \rho_0 g h^3}{\kappa \eta_0}\,, \tag{4}$$

$$Rb = \frac{\Delta\rho_F g h^3}{\kappa \eta_0}\,, \tag{5}$$

where α is the thermal expansivity, T_0 reference temperature, ρ_0 reference density, g gravity acceleration, h model height, κ thermal diffusivity, and η_0 reference viscosity. $\Delta\rho_F$ is the density change due to depletion, which is given by

$$\frac{\mathrm{d}\ln\rho}{\mathrm{d}F_{\%}} = -0.00020 \tag{6}$$

from Schutt and Lesher (2006), where $F_{\%} = 100F$ is the depletion in percentage, and $\rho = \rho_0$ (reference density) when $F_{\%} = 0$. The chosen value of -0.00020 is representative of asthenospheric conditions in our models (about 3 GPa).

The dissipation number is defined as

$$Di = \frac{\alpha g h}{C_p}\,, \tag{7}$$

where C_p is the constant pressure heat capacity of the mantle.

1.1 Viscosity parametrization and water weakening

Viscosity parametrization is linear with temperature dependency (Karato and Wu, 1993):

$$\eta_{dry} = A \exp\left(\frac{E + PV}{RT_{abs}}\right)\,, \tag{8}$$

where A is the rheological pre-exponent, E activation energy, V activation volume, R universal gas constant, and T_{abs} the absolute temperature. We use a low value of activation energy ($E = 150\,\mathrm{kJ/mol}$), in order to mimic the effect of dislocation creep. This is in line with the results of Christensen (1984), who proposes that 50 to 70 percent smaller values of activation enthalpy should be used, and van Hunen et al. (2005) who found that value $E = 120\,\mathrm{kJ/mol}$ produces similar lithospheric erosion effect to nonlinear viscosity models.

The effective hydrous viscosity

$$\eta_{hydrous} = W \eta_{dry} \tag{9}$$

with

$$W = 100^{\frac{-X_{H2O}}{X_{H2O+a}}} \tag{10}$$

produces exponential viscosity decrease and maximum weakening of two orders of magnitude (compared to the dry mantle), compatible with experimental results showing that for olivine aggregates the strain rate $\dot{\epsilon} \propto f_{H_2O}^r$, that is, the viscosity $\eta \propto f_{H_2O}^{-r}$, where r is constant, and f_{H_2O} is the water fugacity (Bai and Kohlstedt, 1992; Mei and Kohlstedt, 2000; Hirth and Kohlstedt, 2003). The experimental results have, to some extent, constrained the values of the exponent r (about 1.0 ± 0.2), the relationship between water content and water fugacity (nearly linear at low olivine water contents), and the partitioning of bulk water content between mantle minerals. However, uncertainties related to the effect of water on mantle rheology still remain, and by using a simpler relationship (eq. 10), we can adjust the sensitivity of mantle rheology to the water content in our models to more easily perform parameter studies. Additional advantage of our formulation is that, whereas in experimentally constrained relationships, two rheologies are needed (one for dry, one for hydrous rheology, because in hydrous rheology law viscosity approaches infinity as water fugacity approaches zero), we can model both wet and dry or nearly dry cases using the same law.

Symbol	Definition	Value
L	Latent heat of melt	$560\,\mathrm{kJ\,kg^{-1}}$
α	Coefficient of thermal expansion	$3.5 \cdot 10^{-5}\,\mathrm{K^{-1}}$
T_0	Reference temperature	1350°C
ρ_0	Reference density	$3300\,\mathrm{kg\,m^{-3}}$
h	Model height	660 km
κ	Thermal diffusivity	$10^{-6}\,\mathrm{m^2 s^{-1}}$
η_0	Reference viscosity	$10^{22}\,\mathrm{Pa\,s}$
C_p	Constant pressure heat capacity	$1250\,\mathrm{J\,kg^{-1}\,K^{-1}}$
A	Rheological pre-exponent	$1.82 \cdot 10^{14}\,\mathrm{Pa\,s}$
E	Activation energy	$150\,\mathrm{kJ\,mol^{-1}}$
V	Activation volume	$4\,\mathrm{cm^3\,mol^{-1}}$
a	Viscosity's sensitivity to water	200–500 ppm
X_{H_2O}	Mantle water content	200–600 ppm

Used model parameters and their dimensional values.

The range of a used in the models is determined by two factors: The lower boundary is chosen so that ambient mantle water contents (outside subduction modified regions) would not cause too high viscosity weakening, thus limiting the lower boundary to values clearly larger than 120 ppm (approximate MORB source region water contents). The upper boundary is chosen such that results with higher values do not significantly differ from the highest value used. This indifference of results to parameter a happens because as a grows, the form of W approaches linearity, and the greatest variation in the form of W is seen when values of a are in the range from zero to about 500 ppm.

1.2 Benchmarking

The code used has been succesfully benchmarked against the results of Blankenbach et al. (1989) (Boussinesq approximation) and King et al. (2010) (Extended Boussinesq approximation).

1.3 Model domain, boundary conditions

Our cartesian model domain is 660 km in height and 2640 km in width (aspect ratio 1:4). All the boundaries are closed with free-slip boundary conditions. Heat flow is zero at the horizontal boundaries, and $T = 0$ (0°C) at the surface and $T = 1.25254$ (1690°C) at the bottom. Initial temperature field is provided by running one of the models ($X_{H_2O} = 200$ ppm, $a = 200$ ppm) for > 300 Ma model time to a statistical steady state, with melting disabled, resulting in a more or less flat, approximately 100 km thick high viscosity lithosphere, and restarting this model with new values of X_{H_2O} and a and with melting enabled. The initial temperature field has a mantle potential temperature of about 1300°C.

Model domain has been discretized in to 256 elements in x-direction and 128 elements in z-direction.

1.4 Processing of numerical results

The melt generation within the mantle has been recorded, excluding the proximity of horizontal boundaries, where closed boundaries tend to produce anomalously strong upwelling in some models, leading to high decompressional melting rate.

We analyze the resulting crust production array (rate of melting plotted against time on x-axis and location on y-axis) using multivariate (2D) Fast Fourier Transformation (FFT). For this we use the `fft` routine of the statistical computing software `R` (R Core Team, 2013; Singleton, 1979). Except for very low crust production models, the FFTs show clear maxima between 0.2 to 0.0 1/Ma (5 to Infinite Ma) and between 0.007 and 0.002 1/km (140 km to 500 km) (e.g. Figure S1). The point of maximum amplitude vary slightly among models but with no clear systematics. All models with enough crust production (more than about 50 m average overall crustal production after 40 Myrs) to do the FFT analysis, show a maximum at 0.005 1/km (200 km spatial wavelength), and the location of this maximum on the x-axis (time) vary between 0.05 1/Ma and 0.2 1/Ma (5 to 20 Ma temporal wavelength).

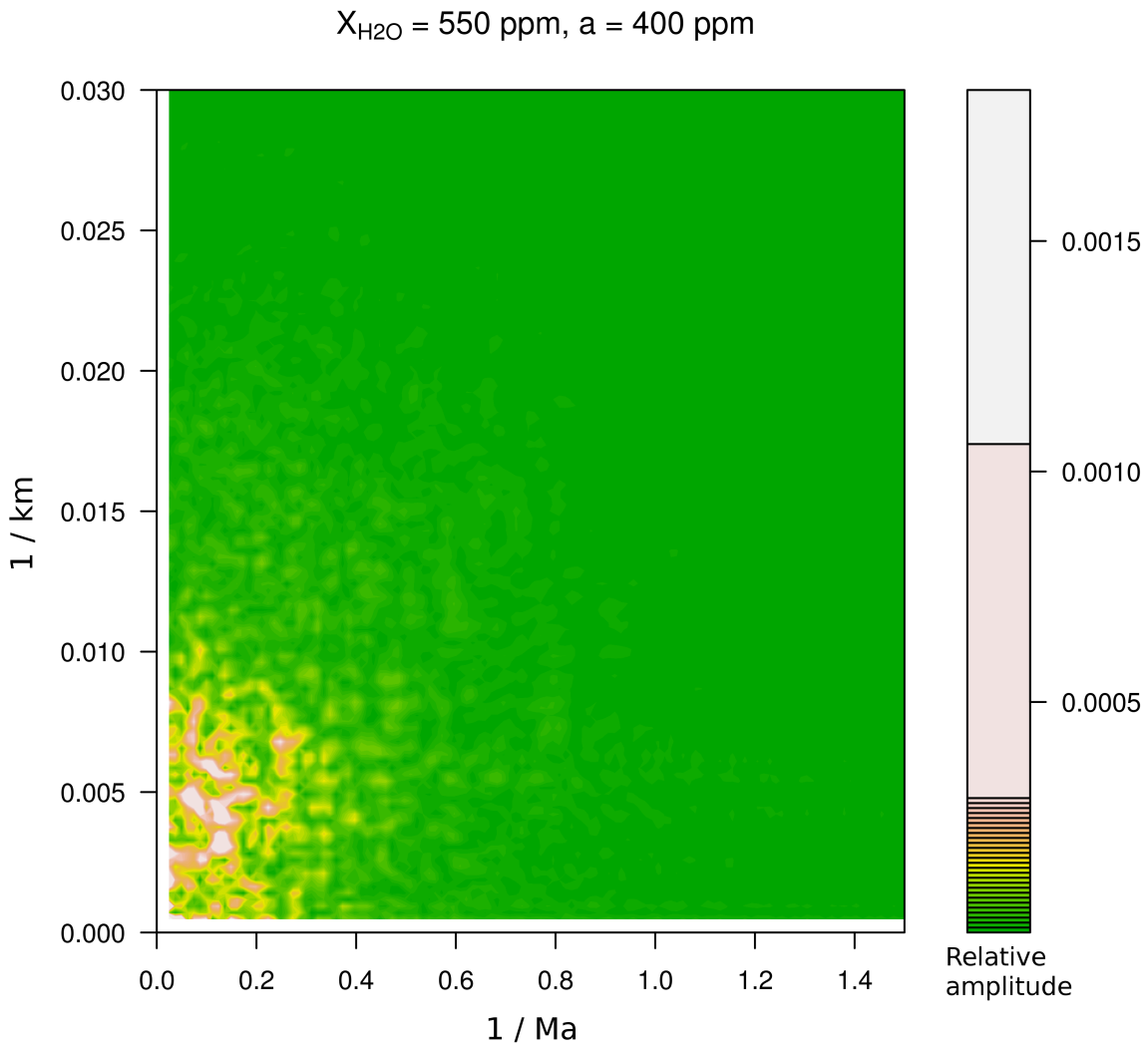

Figure S1: 2D FFT of the crust production array for the model $X_{H2O} = 550\,\text{ppm}$, $a = 400\,\text{ppm}$.

References

Bai, Q., Kohlstedt, D., May 1992. High-temperature creep of olivine single crystals, 2. dislocation structures. Tectonophysics 206 (1-2), 1–29.
URL http://linkinghub.elsevier.com/retrieve/pii/004019519290365D

Blankenbach, B., Busse, F., Christensen, U., Cserepes, L., Gunkel, D., Hansen, U., Harder, H., Jarvis, G., Koch, M., Marquart, G., Moore, D., Olson, P., Schmeling, H., Schnaubelt, T., 1989. A benchmark comparison for mantle convection codes. Geophysical Journal International 98 (1989), 23–38.

Christensen, U., 1984. Convection with pressure- and temperature-dependent non-Newtonian rheology. Geophysical Journal of the Royal Astronomical Society 77, 343–384.

Christensen, U. R., Yuen, D. A., 1985. Layered Convection Induced by Phase Transitions. Journal of Geophysical Research 90 (B12), 10291–10300.

Gerya, T. V., Yuen, D. a., Dec. 2003. Characteristics-based marker-in-cell method with conservative finite-differences schemes for modeling geological flows with strongly variable transport properties. Physics of the Earth and Planetary Interiors 140 (4), 293–318.
URL http://linkinghub.elsevier.com/retrieve/pii/S0031920103001900

Hirth, G., Kohlstedt, D., 2003. Rheology of the Upper Mantle and the Mantle Wedge: A view from the Experimentalists. Geophysical Monograph 183, 83–105.

Karato, S.-I., Wu, P., 1993. Rheology of the Upper Mantle: A Synthesis. Science 260 (5109), 771–778.

King, S. D., Lee, C., van Keken, P. E., Leng, W., Zhong, S., Tan, E., Tosi, N., Kameyama, M. C., 2010. A community benchmark for 2-D Cartesian compressible convection in the Earth's mantle.

Mei, S., Kohlstedt, D., 2000. Influence of water on plastic deformation of olivine aggregates 1 . Diffusion creep regime. Journal of Geophysical Research 105, 21457–21469.

Moresi, L., Gurnis, M., 1996. Constraints on the lateral strength of slabs from three-dimensional dynamic flow models. Earth and Planetary Science Letters 138, 15–28.

R Core Team, 2013. R: A Language and Environment for Statistical Computing. R Foundation for Statistical Computing, Vienna, Austria.
URL http://www.r-project.org

Schutt, D. L., Lesher, C. E., 2006. Effects of melt depletion on the density and seismic velocity of garnet and spinel lherzolite. Journal of Geophysical Research 111 (B5), 1–24.
URL http://www.agu.org/pubs/crossref/2006/2003JB002950.shtml

Singleton, R. C., 1979. Mixed Radix Fast Fourier Transforms. In: Committee, I. D. S. P. (Ed.), Programs for digital signal processing. IEEE Press, New York.

van Hunen, J., Zhong, S., Shapiro, N., Ritzwoller, M., Sep. 2005. New evidence for dislocation creep from 3-D geodynamic modeling of the Pacific upper mantle structure. Earth and Planetary Science Letters 238 (1-2), 146–155.
URL http://linkinghub.elsevier.com/retrieve/pii/S0012821X05004619

Zhong, S., Zuber, M. T., Moresi, L., Gurnis, M., 2000. Role of temperature-dependent viscosity and surface plates in spherical shell models of mantle convection. Journal of Geophysical Research 105 (B5), 11063–11082.

2 Volcanism of the Turkish-Iranian plateau

2.1 Numeric ages and their sources

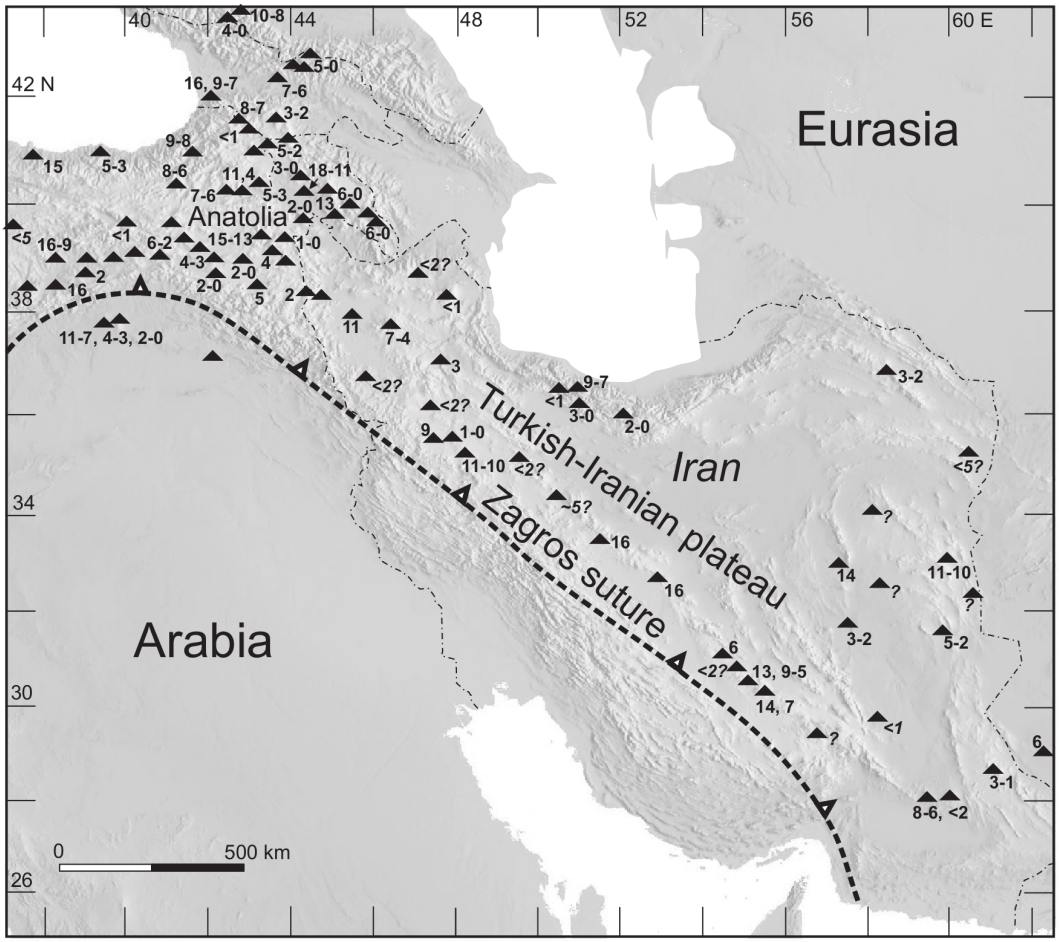

Figure S2: Ages of the volcanic centres shown in Figure 1 in the main text.

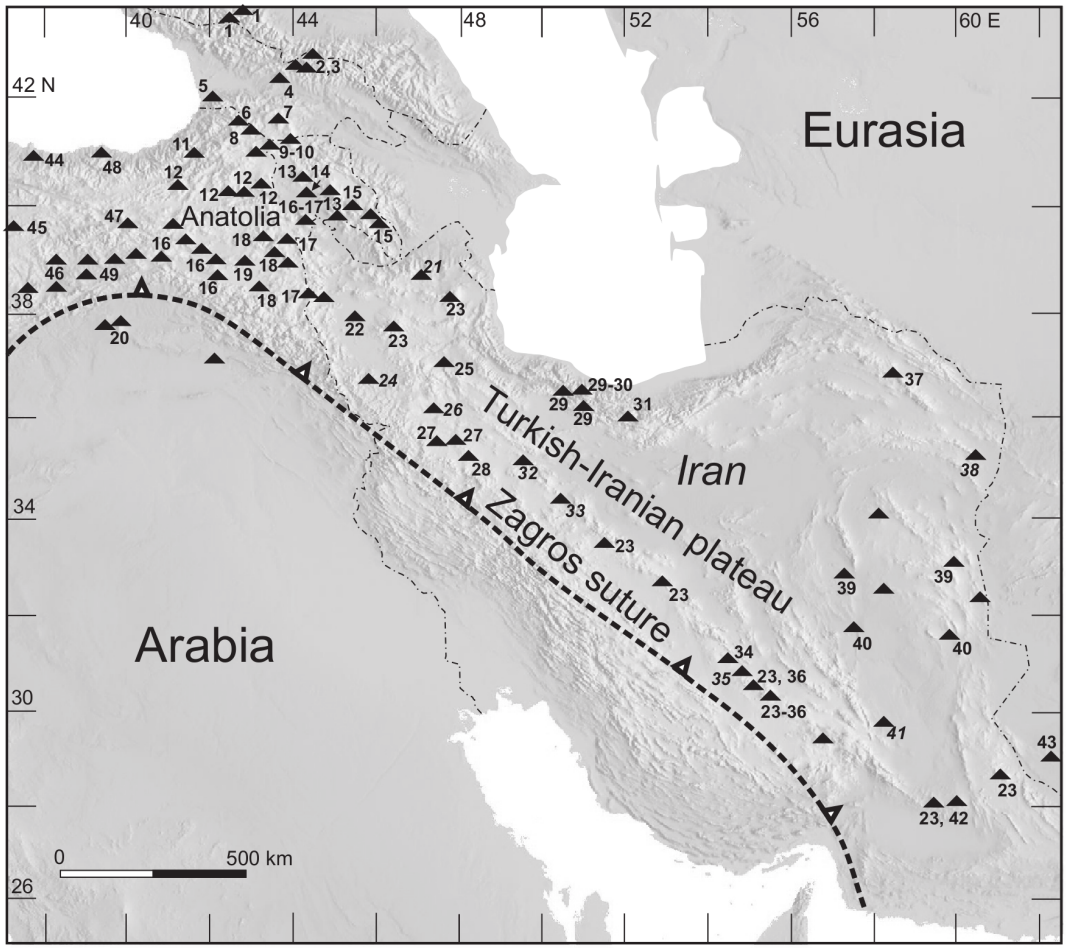

Figure S3: References of the volcanic centre ages shown in Figure S2 and Figure 1 in the main text.

Sources for the ages / references in Figure S2/S3:

1 – Lebedev et al (2006)	26 – Zahedi and Hajian (1985)
2 – Lebedev et al (2006)	27 – Boccaletti et al (1976)
3 – Lebedev et al (2011)	28 – Richards et al (2006)
4 – Lebedev et al (2013)	29 – Guest et al (2007)
5 – Lebedev et al (2009)	30 – Axen et al (2001)
6 – Lebedev et al (2012)	31 – Davidson et al (2004)
7 – Lebedev et al (2007)	32 – Alai-Mahabadi and Khalatbari-Jafari (2003)
8 – Chernyshev et al (2006)	33 – Emami (1981)
9 – Lebedev et al (2008a)	34 – Kouhestani et al (2012)
10 – Lebedev et al (2008b)	35 – Djokovic et al (1973)
11 – Eyuboglu et al (2012)	36 – McInnes et al (2005)
12 – Keskin et al (1998)	37 – Shabanian et al (2009)
13 – Mitchell and Westaway (1999)	38 – Saadat and Stern (2012)
14 – Karapetian et al (2001)	39 – Pang et al (2012)
15 – Arutyunyan et al (2007)	40 – Walker et al (2009)
16 – Pearce et al (1990)	41 – Milton (1977)
17 – Allen et al (2011)	42 – Saadat and Stern (2011)
18 – Lebedev et al (2010)	43 – Richards et al (2012)
19 – Innocenti et al (1976)	44 – Temizel et al (2012)
20 – Keskin et al (2012)	45 – Parlak et al (2001)
21 – Dabiri et al (2011)	46 – Kurum et al (2008)
22 – Pang et al (2013)	47 – Karsli et al (2008)
23 – Chiu et al (2013)	48 – Aydin et al (2008)
24 – Eftekharnezhad (1973)	49 – Arger et al (2000)
25 – Hassanzadeh et al (2008)	

2.2 References

Alai-Mahabadi, S., and Khalatbari-Jafari, B. M., 2003, Noubaran: Geological survey of Iran, scale 1:100,000.

Allen, M. B., Mark, D. F., Kheirkhah, M., Barfod, D., Emami, M. H., and Saville, C., 2011, 40Ar/39Ar dating of Quaternary lavas in northwest Iran: constraints on the landscape evolution and incision rates of the Turkish-Iranian plateau: Geophysical Journal International, v. 185, no. 3, p. 1175-1188.

Arger, J., Mitchell, J., and Westaway, R. W. C., 2000, Neogene and Quaternary volcanism of southeastern Turkey, in Bozkurt, E., Winchester, J. A., and Piper, J. D. A., eds., Tectonics and Magmatism in Turkey and the Surrounding Area, Volume 173: London, Geological Society, London, p. 459-487.

Arutyunyan, E. V., Lebedev, V. A., Chernyshev, I. V., and Sagatelyan, A. K., 2007, Geochronology of Neogene-Quaternary volcanism of the Geghama Highland (Lesser Caucasus, Armenia): Doklady Earth Sciences, v. 416, no. 7, p. 1042-1046.

Axen, G. J., Lam, P. S., Grove, M., Stockli, D. F., and Hassanzadeh, J., 2001, Exhumation of the west-central Alborz Mountains, Iran, Caspian subsidence, and collision-related tectonics: Geology, v. 29, p. 559-562.

Aydin, F., Karsli, O., and Chen, B., 2008, Petrogenesis of the Neogene alkaline volcanics with implications for post-collisional lithospheric thinning of the Eastern Pontides, NE Turkey: Lithos, v.104, p.249-266.

Boccaletti, M., Innocenti, F., Manetti, P., Mazzuoli, R., Motamed, A., Pasquare, G., Radicati di Brozolo, F., and Amin Sobhani, E., 1976, Neogene and quaternary volcanism of the Bijar Area (Western Iran): Bulletin of Volcanology, v. 40, p. 122-132.

Chernyshev, I. V., Lebedev, V. A., and Arakelyants, M. M., 2006, K-Ar dating of quaternary volcanics: Methodology and interpretation of results: Petrology, v. 14, no. 1, p. 62-80.

Chiu, H. Y., Chung, S. L., Zarrinkoub, M. H., Mohammadi, S. S., Khatib, M. M., and Iizuka, Y., 2013, Zircon U-Pb age constraints from Iran on the magmatic evolution related to Neotethyan subduction and Zagros orogeny: Lithos, v. 162-163, p. 70-87.

Dabiri, R., Emami, M. H., Mollaei, H., Chen, B., Abedini, M. V., Omran, N. R., and Ghaffari, M., 2011, Quaternary post-collision alkaline volcanism NW of Ahar (NW Iran): geochemical constraints of fractional crystallization process: Geologica Carpathica, v. 62, no. 6, p. 547-562.

Davidson, J., Hassanzadeh, J., Berzins, R., Stockli, D. F., Bashukooh, B., Turrin, B., and Pandamouz, A., 2004, The geology of Damavand volcano, Alborz Mountains, northern Iran: Geological Society Of America Bulletin, v. 116, no. 1-2, p. 16-29.

Djokovic, I., Cvetic, S., and Dimitrijevic, M. D., 1973, Dehaj: Geological Survey of Iran, scale 1:100,000.

Eftekharnezhad, J., 1973, Geological Map of Mahabad: Geological Survey of Iran Press, scale 1:250,000.

Emami, M. H., 1981, Geological Quadrangle map of Iran, 1:250,000 scale, sheet E6 (Qom), Geological Survey of Iran.

Eyuboglu, Y., Santosh, M., Yi, K., Bektas, O., and Kwon, S., 2012, Discovery of Miocene adakitic dacite from the Eastern Pontides Belt (NE Turkey) and a revised geodynamic model for the late Cenozoic evolution of the Eastern Mediterranean region: Lithos, v. 146, p. 218-232.

Guest, B., Horton, B. K., Axen, G. J., Hassanzadeh, J., and McIntosh, W. C., 2007, Middle to late Cenozoic basin evolution in the western Alborz Mountains: Implications for the onset of collisional deformation in northern Iran: Tectonics, v. 26, DOI: 10.1029/2006TC002091.

Hassanzadeh, J., Stockli, D. F., Horton, B. K., Axen, G. J., Stockli, L. D., Grove, M., Schmitt, A. K., and Walker, J. D., 2008, U-Pb zircon geochronology of late Neoproterozoic-Early Cambrian granitoids in Iran: Implications for paleogeography, magmatism, and exhumation history of Iranian basement: Tectonophysics, v. 451, no. 1-4, p. 71-96.

Innocenti, F., Mazzuoli, R., Pasquare, G., Radicatidibrozolo, F., and Villari, L., 1976, Evolution of volcanism in area of interaction between Arabian, Anatolian and Iranian plate (Lake Van, eastern Turkey): Journal of Volcanology and Geothermal Research, v. 1, no. 2, p. 103-112.

Karapetian, S. G., Jrbashian, R. T., and Mnatsakanian, A. K., 2001, Late collision rhyolitic volcanism in the north-eastern part of the Armenian Highland: Journal of Volcanology and Geothermal Research, v. 112, p. 189-220.

Karsli, O., Chen, B., Uysal, I., Aydin, F., Wijbrans, J. R., and Kandemir, R., 2008, Elemental and Sr-Nd-Pb isotopic geochemistry of the most recent Quaternary volcanism in the Erzincan Basin, Eastern Turkey: framework for the evaluation of basalt-lower crust interaction: Lithos, v. 106, no. 1-2, p. 55-70.

Keskin, M., Chugaev, A. V., Lebedev, V. A., Sharkov, E. V., Oyan, V., and Kavak, O., 2012, The geochronology and origin of mantle sources for late cenozoic intraplate volcanism in the frontal part of the Arabian plate in the Karacadag neovolcanic area of Turkey. Part 1. The results of isotope-geochronological studies: Journal of Volcanology and Seismology, v. 6, no. 6, p. 352-360.

Keskin, M., Pearce, J. A., and Mitchell, J. G., 1998, Volcano-stratigraphy and geochemistry of collision-related volcanism on the Erzurum-Kars Plateau, northeastern Turkey: Journal of Volcanology and Geothermal Research, v. 85, p. 355-404.

Kouhestani, H., Ghaderi, M., Zaw, K., Meffre, S., and Emami, M. H., 2012, Geological setting and timing of the Chah Zard breccia-hosted epithermal gold-silver deposit in the Tethyan belt of Iran: Mineralium Deposita, v. 47, no. 4, p. 425-440.

Kurum, S., Onal, A., Boztug, D., Spell, T., and Arslan, M., 2008, (40)Ar/(39)Ar age and geochemistry of the post-collisional Miocene Yamadag volcanics in the Arapkir area (Malatya Province), eastern Anatolia, Turkey: Journal of Asian Earth Sciences, v. 33, no. 3-4, p. 229-251.

Lebedev, V. A., Bubnov, S. N., Chernyshev, I. V., Chugaev, A. V., Dudauri, O. Z., and Vashakidze, G. T., 2007, Geochronology and genesis of subalkaline basaltic lava rivers at the Dzhavakheti highland, Lesser Caucasus: K-Ar and Sr-Nd isotopic data: Geochemistry International, v. 45, no. 3, p. 211-225.

Lebedev, V. A., Bubnov, S. N., Chernyshev, I. V., and Gol'tsman, Y. V., 2006a, Basic magmatism in the geological history of the Elbrus neovolcanic area, Greater Caucasus: Evidence from K-Ar and Sr-Nd isotope data: Doklady Earth Sciences, v. 406, no. 1, p. 37-40.

Lebedev, V. A., Bubnov, S. N., Chernyshev, I. V., Gol'tsman, Y. V., Chugaev, A. V., and Vashakidze, G. T., 2006b, Pliocene granitoid massif in the Kazbek volcanic center: First geochronological and isotope-geochemical data: Doklady Earth Sciences, v. 411, no. 9, p. 1393-1397.

Lebedev, V. A., Bubnov, S. N., Dudauri, O. Z., and Vashakidze, G. T., 2008a, Geochronology of Pliocene volcanism in the Dzhavakheti Highland (the Lesser Caucasus). Part 1: Western part of the Dzhavakheti Highland: Stratigraphy and Geological Correlation, v. 16, no. 2, p. 204-224.

-, 2008b, Geochronology of Pliocene volcanism in the Dzhavakheti Highland (the Lesser Caucasus). Part 2: Eastern part of the Dzhavakheti Highland. Regional geological correlation: Stratigraphy and Geological Correlation, v. 16, no. 5, p. 553-574.

Lebedev, V. A., Chernyshev, I. V., Dudauri, O. Z., Vashakidze, G. T., Goltsman, Y. V., Bairova, E. D., and Yakushev, A. I., 2013, Manifestations of Miocene acid intrusive magmatism on the southern slope of the Greater Caucasus: First evidence from isotope geochronology: Doklady Earth Sciences, v. 450, no. 1, p. 550-555.

Lebedev, V. A., Chernyshev, I. V., and Sharkov, E. V., 2011, Geochronological scale and evolution of late Cenozoic magmatism within the Caucasian segment of the alpine belt: Doklady Earth Sciences, v. 441, no. 2, p. 1656-1660.

Lebedev, V. A., Chernyshev, I. V., Vashakidze, G. T., Gudina, M. V., and Yakushev, A. I., 2012, Geochronology of miocene volcanism in the northern part of the Lesser Caucasus (Erusheti Highland, Georgia): Doklady Earth Sciences, v. 444, no. 1, p. 585-590.

Lebedev, V. A., Sakhno, V. G., and Yakushev, A. I., 2009, Late Cenozoic volcanic activity in western Georgia: Evidence from new isotope geochronological data: Doklady Earth Sciences, v. 427, no. 1, p. 819-825.

McInnes, B. I. A., and Evans, N. J., 2005, Application of thermochronology to hydrothermal ore deposits: Low-Temperature Thermochronology: Techniques, Interpretations, and Applications, v. 58, p. 467-498.

Milton, D. J., 1977, Qal'eh Hasan Ali Maars, central Iran: Bulletin of Volcanology, v. 40, p. 201–208.

Mitchell, J., and Westaway, R., 1999, Chronology of Neogene and Quaternary uplift and magmatism in the Caucasus: constraints from K-Ar dating of volcanism in Armenia: Tectonophysics, v. 304, no. 3, p. 157-186.

Pang, K. N., Chung, S. L., Zarrinkoub, M. H., Lin, Y. C., Lee, H. Y., Lo, C. H., and Khatib, M. M., 2013, Iranian ultrapotassic volcanism at ~11 Ma signifies the initiation of post-collisional magmatism in the Arabia–Eurasia collision zone: Terra Nova, v. 25, p. 405-413.

Pang, K. N., Chung, S. L., Zarrinkoub, M. H., Mohammadi, S. S., Yang, H. M., Chu, C. H., Lee, H. Y., and Lo, C. H., 2012, Age, geochemical characteristics and petrogenesis of Late Cenozoic intraplate alkali basalts in the Lut-Sistan region, eastern Iran: Chemical Geology, v. 306, p. 40-53.

Parlak, O., Delaloye, M., Demirkol, C., and Unlugenc, U. C., 2001, Geochemistry of Pliocene/Pleistocene basalts along the Central Anatolian Fault Zone (CAFZ), Turkey: Geodinamica Acta, v. 14, no. 1-3, p. 159-167.

Pearce, J. A., Bender, J. F., Delong, S. E., Kidd, W. S. F., Low, P. J., Guner, Y., Sargolu, F., Yilmaz, Y., Moorbath, S., and Mitchell, J. G., 1990, Genesis of collision volcanism in eastern Anatolia, Turkey: Journal of Volcanology and Geothermal Research, v. 44, p. 189-229.

Richards, J. P., Spell, T., Rameh, E., Razique, A., and Fletcher, T., 2012, High Sr/Y Magmas Reflect Arc Maturity, High Magmatic Water Content, and Porphyry Cu +/- Mo +/- Au Potential: Examples from the Tethyan Arcs of Central and Eastern Iran and Western Pakistan: Economic Geology, v. 107, no. 2, p. 295-332.

Richards, J. P., Wilkinson, D., and Ullrich, T., 2006, Geology of the Sari Gunay epithermal gold deposit, northwest Iran: Economic Geology, v. 101, no. 8, p. 1455-1496.

Saadat, S., and Stern, C. R., 2011, Petrochemistry and genesis of olivine basalts from small monogenetic parasitic cones of Bazman stratovolcano, Makran arc, southeastern Iran: Lithos, v. 125, p. 607-619.

Saadat, S., and Stern, C. R., 2012, Petrochemistry of a xenolith-bearing Neogene alkali olivine basalt from northeastern Iran: Journal of Volcanology and Geothermal Research, v. 225, p. 13-29.

Shabanian, E., Bellier, O., Siame, L., Arnaud, N., Abbassi, M. R., and Cocheme, J. J., 2009, New tectonic configuration in NE Iran: Active strike-slip faulting between the Kopeh Dagh and Binalud mountains: Tectonics, v. 28, TC5002, doi: 10.1029/2008TC002444.

Temizel, I., Arslan, M., Ruffet, G., and Peucat, J. J., 2012, Petrochemistry, geochronology and Sr-Nd isotopic systematics of the Tertiary collisional and post-collisional volcanic rocks from the Ulubey (Ordu) area, eastern Pontide, NE Turkey: Implications for extension-related origin and mantle source characteristics: Lithos, v. 128, p. 126-147.

Walker, R. T., Gans, P., Allen, M. B., Jackson, J., Khatib, M., Marsh, N., and Zarrinkoub, M., 2009, Late Cenozoic volcanism and rates of active faulting in eastern Iran: Geophyical Journal International, v. 177, p. 783-805.

Zahedi, M., and Hajian, J., 1985, Sanandaj: Geological Survey of Iran, scale 1:250,000.